

Jonsdottir Thorey (Orcid ID: 0000-0002-0618-4731)
Counihan Natalie (Orcid ID: 0000-0002-8973-3344)

Characterisation of complexes formed by parasite proteins exported into the host cell compartment of *Plasmodium falciparum* infected red blood cells.

Authors Thorey K. Jonsdottir^{1,2#}, Natalie A. Counihan³, Joyanta K. Modak³, Betty Kouskousis^{1,4}, Paul R. Sanders¹, Mikha Gabriela^{1,3}, Hayley E. Bullen¹, Brendan S. Crabb^{1,2,5}, Tania F. de Koning-Ward³ and Paul R. Gilson^{1#}.

¹Burnet Institute, Melbourne, Australia

²Department of Microbiology and Immunology, University of Melbourne, Australia

³School of Medicine, Deakin University, Waurn Ponds, Australia

⁴Monash Micro-imaging, Monash University, Australia

⁵Department of Microbiology, Monash University, Australia.

Correspondence #

Thorey K. Jonsdottir and Paul R. Gilson, Burnet Institute, Melbourne, Australia.

E-mail thorey.jonsdottir@burnet.edu.au, paul.gilson@burnet.edu.au; Tel. (+61) 385062481

Funding Information

University of Melbourne Research Scholarship, Deakin University Postgraduate Research Scholarship, Deakin University HAtCH funding.

Keywords. Malaria, *Plasmodium falciparum*, exported proteins, Maurer's clefts, J-dots, RhopH, new permeability pathways

Take aways

- New protein complexes were identified that provide a clearer picture of the *Plasmodium falciparum* exported protein network.

This article has been accepted for publication and undergone full peer review but has not been through the copyediting, typesetting, pagination and proofreading process which may lead to differences between this version and the [Version of Record](#). Please cite this article as doi: [10.1111/cmi.13332](https://doi.org/10.1111/cmi.13332)

- Five proteins were confirmed to interact with RhopH components: RESA1, PF3D7_1201000, PF3D7_0401800, LyMP and PF3D7_1401200.
- The export and localisation of six new proteins previously hypothesised to be exported into the red blood cell cytoplasm were validated by immunofluorescence analysis.

Summary

During its intraerythrocytic life cycle, the human malaria parasite *Plasmodium falciparum* supplements its nutritional requirements by scavenging substrates from the plasma through the new permeability pathways (NPPs) installed in the red blood cell (RBC) membrane. Parasite proteins of the RhopH complex: CLAG3, RhopH2, RhopH3, have been implicated in NPP activity. Here we studied 13 exported proteins previously hypothesised to interact with RhopH2, to study their potential contribution to the function of NPPs. NPP activity assays revealed that the 13 proteins do not appear to be individually important for NPP function, as conditional knockdown of these proteins had no effect on sorbitol uptake. Intriguingly, reciprocal immunoprecipitation assays showed that five of the 13 proteins interact with all members of the RhopH complex, with PF3D7_1401200 showing the strongest association. Mass spectrometry-based proteomics further identified new protein complexes; a cytoskeletal complex and a Maurer's clefts/J-dot complex, which overall helps clarify protein-protein interactions within the infected RBC (iRBC) and is suggestive of the potential trafficking route of the RhopH complex itself to the RBC membrane.

Introduction

Malaria is a febrile illness caused by *Plasmodium* parasites. It remains a major global health problem and was estimated to cause 229 million cases in 2019, leading to the death of approximately half a million people, most of whom were children under the

age of five (W.H.O, 2020). *P. falciparum*, the causative agent of the most severe form of malaria in humans, is renowned for its ability to manipulate and modify the red blood cells (RBCs) of its human host for its survival by exporting hundreds of parasite proteins into the RBC cytosol [reviewed in (de Koning-Ward *et al.*, 2016)]. The infected RBC (iRBC) becomes more rigid and adherent to the microvascular endothelium, preventing its circulation through the spleen and subsequent immune destruction [reviewed in (Tilley *et al.*, 2011)]. Parasite structures are formed in the iRBC to traffic parasite proteins within the host cell. These include Maurer's clefts (MCs) which are membranous structures involved in protein cargo sorting, and J-dots which are mobile structures affiliated with heat shock proteins and trafficking of the major virulence protein PfEMP1 (Lanzer *et al.*, 2006, Kulzer *et al.*, 2010, Kulzer *et al.*, 2012, Behl *et al.*, 2019). The iRBC also becomes more permeable to plasma nutrients including isoleucine and pantothenic acid to supplement rapid parasite growth (Kirk *et al.*, 1994, Kirk *et al.*, 1995, Cooke *et al.*, 2004, Boddey *et al.*, 2013, Gilson *et al.*, 2017).

The establishment of nutrient channels in the iRBC membrane, collectively referred to as the new permeability pathways (NPPs), renders the iRBC permeable to various solutes (Ginsburg *et al.*, 1985, Upston *et al.*, 1995, Staines *et al.*, 2000). These influx/efflux channels allow the parasite to gain access to essential extracellular plasma nutrients [reviewed in (Saliba *et al.*, 2001)], and aid in maintaining optimum physiological stability of the infected host cell (Lew *et al.*, 2003).

Through conditional drug resistance, knockdown studies and nutrient uptake assays, NPP activity has been affiliated with the functioning of three rhoptry proteins, those being RhopH1 (CLAG3) (Nguiragool *et al.*, 2011, Ito *et al.*, 2017), RhopH2 (Counihan *et al.*, 2017, Ito *et al.*, 2017) and RhopH3 (Sherling *et al.*, 2017). RhopH1 is encoded by a multigene family comprising *clag2*, *clag3.1*, *clag3.2*, *clag8* and *clag9*, whilst RhopH2 and RhopH3 are encoded by single genes (Kaneko *et al.*, 2001, Kaneko *et al.*, 2005). The RhopH1 genes *clag3.1* and *clag3.2* are mutually

exclusively transcribed and are the only *clags* affiliated with NPP activity so far, but are not essential for parasite survival (Comeaux *et al.*, 2011, Nguitragool *et al.*, 2011). RhopH2 and RhopH3 are both refractory to genetic disruption (Cowman *et al.*, 2000, Ito *et al.*, 2017) and protein knockdown results in severe growth reduction through decreased nutrient uptake and in the case of RhopH3 knockdown also results in invasion defects (Counihan *et al.*, 2017, Ito *et al.*, 2017, Sherling *et al.*, 2017).

It remains unclear if the RhopH complex alone is sufficient to carry out NPP functions or if other proteins are additionally required (Ito *et al.*, 2017). NPP function has also been shown to depend on the *Plasmodium* translocon of exported proteins (PTEX) (Beck *et al.*, 2014), which resides in the parasitophorous vacuole (PV) and exports proteins across the PV membrane (PVM) and into the host cell (de Koning-Ward *et al.*, 2009). There is conflicting evidence whether the RhopH complex itself requires PTEX for export into the RBC or if other exported proteins are needed for correct NPP functioning (Beck *et al.*, 2014, Ito *et al.*, 2017, Ahmad *et al.*, 2020). It is also unclear how the RhopH complex is delivered from the PV/PVM to the iRBC periphery, but studies have shown that RhopH2 and RhopH3 are needed for the correct trafficking of CLAG3 to the surface (Ito *et al.*, 2017, Ahmad *et al.*, 2020).

A recent study has revealed that RhopH2 co-immunoprecipitates 30 proteins predicted to be exported via PTEX, raising the question of whether these proteins could possess NPP functions as well (Counihan *et al.*, 2017). These exported proteins include *Plasmodium* helical interspersed subtelomeric (PHIST) proteins (Sargeant *et al.*, 2006), MC proteins (Lanzer *et al.*, 2006) and cytoskeletal components. Here we studied 13 of the predicted RhopH2-interacting exported proteins to confirm their potential role in NPP function and affiliation with RhopH components. Sorbitol-based NPP assays together with conditional protein knockdown assays revealed that none of the 13 proteins appear to play a major role in NPP functioning. However, reciprocal immunoprecipitation assays show that five

of the selected exported proteins co-precipitate RhopH components, four of which also interact with cytoskeletal components. Furthermore, we have expanded the repertoire of known exported proteins to include; PTP4 (PF3D7_0730900), PF3D7_0532300, PF3D7_1477500, Hyp1 (PF3D7_0301600), PF3D7_0113200, PF3D7_0501000 and PF3D7_1401200. Lastly, mass spectrometry-based proteomics analysis for 10 of the exported proteins reveals new networking clusters of exported proteins within the iRBC and identifies potential novel complexes involved in cytoskeletal activity, as well as a transient trafficking hub connecting J-dots and MCs structures. Given the association of RhopH proteins with both MC and J-dot residential proteins we propose that these structures are involved in the trafficking of the RhopH complex to the RBC membrane where the NPPs are established.

Results

Generation of transgenic parasite lines

Here we focus on 13 of the 30 exported proteins found to co-precipitate with RhopH2 (Counihan *et al.*, 2017) (Table S1, grey). Proteins were chosen based on RhopH2 association and the ease of generating the gene constructs. 3D7 transgenic parasite lines were generated using either the selection linked integration (SLI) method (Birnbaum *et al.*, 2017) or via standard homologous recombination techniques (Crabb *et al.*, 1997) (Fig. S1A). Diagnostic PCR was used to confirm that the 13 proteins had been correctly tagged with both a C-terminal HA-epitope tag (for protein detection), and a *glmS* ribozyme (for conditional protein knockdown) (Fig. S1B, C). Subsequent western blots of tagged lines probed with anti-HA revealed that all 13 parasite lines displayed a HA-epitope band of the expected size indicating successful targeting of the genes of interest (Fig. S1D). For the SLI constructs, a band ~30 kDa larger than expected for the protein of interest was often observed, which is likely a fusion of the exported protein and neomycin resistance protein formed as a result of

incomplete ribosome skipping between the two coding sequences that are separated by a 2A sequence (Fig. S1D).

Localisation of the 13 exported proteins within the host cell

Indirect immunofluorescence assays were used to confirm the localisation of the 13 proteins (Fig. 1). RESA1, PF3D7_1201000, PF3D7_0401800, PF3D7_0424600 and LyMP displayed a strong signal at the surface of the iRBC, which was often accompanied by a weaker signal in the cytoplasm (Fig. 1i), in agreement with previous studies (Proellocks *et al.*, 2014, Tarr *et al.*, 2014, Tiburcio *et al.*, 2015, Davies *et al.*, 2016, Moreira *et al.*, 2016). PF3D7_0532300 has been previously suggested to localise to the MCs (Moreira *et al.*, 2016), which we confirm here through co-localisation with the MC marker REX1 but we also observed signal lining the iRBC surface (Fig. 1i). The remainder of the proteins analysed displayed a diffuse or punctate signal throughout the iRBC, with PF3D7_0501000 showing complete co-localisation with REX1 whilst the others showed only partial or no co-localisation with REX1 (Fig. 1ii). Some proteins also showed partial co-localisation with the J-dot resident protein PF3D7_0801000 (Charnaud *et al.*, 2017) (Fig. S2). Super-resolution microscopy was used to gain better resolution of surface protein localisation. RESA, PF3D7_0401800, PF3D7_0424600 and LyMP showed a more continuous signal around the iRBC surface, whereas PF3D7_0532300 and PF3D7_1201000 showed a punctate signal around the surface, indicating they might be restricted to specific zones (Fig. 1i).

Partial knockdown of the 13 exported proteins did not affect NPP activity

To perform functional studies with the 13 proteins, parasites were treated with glucosamine (GlcN), to activate the *glmS* ribozyme, resulting in reduced protein expression (Prommana *et al.*, 2013). Trophozoite iRBCs were treated for one cell cycle \pm 2.5 mM GlcN and subsequent western blots of the GlcN-treated parasites

indicated protein expression was reduced by approximately 40-80% depending on protein, as measured via densitometry (Fig. 2A and S3A).

To assess NPP activity, sorbitol lysis sensitivity was measured (Wagner *et al.*, 2003, Nguitragool *et al.*, 2011, Counihan *et al.*, 2017). Specifically, we transfected the 13 parasite lines with an exported nanoluciferase (Nluc), which can be utilised as a read-out for the percentage parasite lysis following treatment with sorbitol (Fig. 2B) (Azevedo *et al.*, 2014, Counihan *et al.*, 2017). Immunofluorescence assays confirmed the presence of exported Nluc in all 13 lines (Fig. 2C, S3B).

Trophozoite iRBC were treated with increasing concentrations of GlcN for one cycle to knockdown expression of each tagged protein, prior to incubation in isotonic sorbitol lysis buffer containing NanoGlo, the substrate of Nluc. Sorbitol-mediated lysis of iRBCs results in release of the exported Nluc which emits bioluminescence in the presence of NanoGlo and can be used as a direct indicator of NPP activity. We observed no changes in sorbitol lysis sensitivity in relative light units (RLU)/min at any GlcN concentration for the 13 proteins studied when compared to wild type parasites (Fig. 2D, in red). In contrast, RhopH2-HA*gImS* parasites expressing the exported Nluc reporter, exhibited a strong decrease in bioluminescence signal relative to wild type parasites consistent with its involvement in NPP activity (Counihan *et al.*, 2017) (Fig. 2D, in green).

We next assessed if this level of protein knockdown (40-80%) was sufficient to reduce parasite proliferation. Trophozoite-stage parasites were treated with different concentrations of GlcN and harvested each cycle at trophozoites stage over three consecutive cell cycles (seven days). Lactate dehydrogenase (LDH) assays were then performed to measure parasite growth as previously described (Makler *et al.*, 1993a, Persson *et al.*, 2006) and compared to 3D7 parasites (Fig. 2E and S3). Although growth was reduced in the presence of 2.5 mM GlcN over time, only PF3D7_1401200 exhibited significant growth defect by the end of the third cycle of treatment (Fig. 2E, individual graphs for each cycle can be found in Fig. S4).

Immunoprecipitation assays indicate that five proteins co-precipitate RhopH components

The interaction between the 13 proteins and the RhopH complex was validated using reciprocal immunoprecipitation. RBCs infected with trophozoite stage parasites were isolated on magnetic columns and pellets lysed in 0.25% Triton X-100. Lysates were incubated with anti-HA IgG agarose beads and the bound proteins eluted. As a control, wild type 3D7 parasites and transgenic parasites with an irrelevant HA-tagged phosphoglycerate kinase protein (PGK-HA) were used to detect non-specific binding to the anti-HA beads. Interactions were detected by mass spectrometry-based proteomics for 10 proteins (excluding PF3D7_0401800, PF3D7_0501000 and PF3D7_1401200). Peptide counts were used to semi-quantitatively determine the degree of protein-protein interaction as well as protein coverage (Fig. 3A, Table 1 and S2).

When taken together, peptide count and protein coverage indicated that RESA1, 0532300, 1201000 and LyMP co-precipitated all three members of the RhopH complex, whilst the remainder demonstrated association with either RhopH2 only, or no association with any RhopH components (Fig. 3A, Table 1 and S2). To confirm our mass spectrometry analysis, we completed more stringent immunoprecipitation assays using 1% Triton X-100 to see if the association of these four proteins to RhopH complex was strong and detectable by western blotting (Fig. 3Bi). Western blot analysis was completed for RESA1, PF3D7_0532300, PF3D7_1201000, LyMP, PF3D7_0401800, PF3D7_0501000 and PF3D7_1401200. Blots were probed with antibodies specific for RhopH2, CLAG3 and RhopH3 (see antibody specificity Fig. S5) to determine interactions between each of the proteins.

These assays revealed that PF3D7_1401200 showed the strongest association with all RhopH components. RESA1, PF3D7_1201000, PF3D7_0401800 and LyMP also showed interaction with RhopH components but to lesser extent (Fig.

3Bi and S6). PF3D7_0532300 and PF3D7_0501000 showed no interaction with RhopH components when compared to control lines, indicating that the PF3D7_0532300/RhopH interaction is lost when using a stronger detergent concentration. None of the five proteins showed strong interaction with RhopH3.

CLAG3 immunoprecipitation confirms the interaction of RESA1, PF3D7_1201000, PF3D7_0401800, LyMP and PF3D7_1401200

CLAG3 was used to further confirm the association of these five exported proteins with RhopH components. CLAG3.2 was tagged with HA*gImS* using standard homologous recombination techniques as described above (Fig. S1A and B), targeted for immunoprecipitation and analysed via mass spectrometry. Parasitised RBC were lysed in 1% TX100 to identify strong associations. Mass spectrometry analysis revealed that RESA1, PF3D7_1201000, PF3D7_0401800, LyMP and PF3D7_1401200 co-precipitated with CLAG3, whilst PF3D7_0532300 showed no interaction with CLAG3 (Table 1A and S2). These results further confirm our western blot analysis (Fig. 3Bi, S6).

Comparative immunoprecipitation assays identify two new protein complexes - a cytoskeletal complex and a Maurer's cleft/J-dot trafficking complex

Reciprocal immunoprecipitation data clarified certain protein-protein interactions occurring within the iRBC cytoplasm and the potential trafficking route of the RhopH complex. The mass spectrometry analysis strongly suggests that RESA1 and PF3D7_1201000 are in a complex together as they show almost identical protein-protein interactions (Fig. 4.i, Table 1B and S2). Both proteins interact strongly with MESA and PF3D7_0936800 and could therefore be in a cytoskeletal (CS) complex given their localisation within the RBC (Fig. 4i, Fig. 5, Table 1B and S2).

Both RhopH2 (Counihan *et al.*, 2017) and CLAG3 co-immunoprecipitations indicate that GBP130 strongly interacts with both components (Fig. 4i, Table S2). To

confirm this, we utilised an antibody against GBP130 for co-immunoprecipitation assays of magnet purified wild type 3D7 parasites. Western blot analysis revealed that GBP130 was only able to co-precipitate RhopH3 and not the remainder of the RhopH components as would be expected from the mass spectrometry analysis (Fig. 3Bii). GBP130 might be co-precipitating indirectly with RhopH2 and CLAG3 due to their association with RhopH3, which is detectable by mass spectrometry but not by western blotting or this could be due to different antibodies used.

Both PF3D7_0532300 and PF3D7_0301700 are likely to serve a trafficking role within the iRBC as both proteins strongly interact with most of the exported proteins on the list, especially the J-dot chaperones HSP70-x and PF3D7_0801000. Both proteins also strongly associate with the MC resident protein PF3D7_0702500 and these five proteins therefore could potentially form a J-dot and MC (JAM) transient complex involved in protein trafficking (Fig. 4.ii, Table 1C and S2). We also note that PF3D7_0532300 strongly co-precipitated the MC protein REX1 and the major virulence protein PfEMP1 as well as the RBC protein myosin whilst the rest of the proteins showed little or no association with these proteins (Table S2).

Discussion

Here we confirm previous observations for the localisation of: RESA1, PF3D7_0401800, PF3D7_0424600, PF3D7_1201000, LyMP, PF3D7_0301700 (Fig. 5) (Proellocks *et al.*, 2014, Tarr *et al.*, 2014, Schulze *et al.*, 2015, Tiburcio *et al.*, 2015, Davies *et al.*, 2016, Moreira *et al.*, 2016). Furthermore, we have also been able to confirm the prediction studies suggesting that PF3D7_0532300, PTP4, PF3D7_1477500, Hyp1, PF3D7_0113200, PF3D7_0501000 and PF3D7_1401200 are exported into the host cell cytoplasm, and demonstrate that they have diffuse or punctate localisation. One protein, PF3D7_0501000, showed complete co-localisation with REX1 and therefore is an MC resident protein, confirming previous co-precipitation data (Fig. 1, 5) (McHugh *et al.*, 2020).

Knockdown of the 13 proteins had no effect on sorbitol uptake through the NPPs indicating they are not essential for NPP activity at the knockdown levels achieved in this study (Fig. 2A, D). We further used growth assays to assess parasite proliferation during protein knockdown over three consecutive life cycles and determined that PF3D7_1401200 was the only protein with a growth phenotype when compared to wild type parasites (Fig. 2E). Consistently, PF3D7_1401200 is also the only protein out of the 13 proteins shown to be essential through *piggyBac* transposon mutagenesis screen (Zhang *et al.*, 2018).

The 13 proteins were targeted for reciprocal immunoprecipitation to confirm their interaction with RhopH components. We also targeted CLAG3, a RhopH component, for immunoprecipitation analysis to strengthen our findings. When combining all our immunoprecipitation data, five proteins were confirmed as *bona fide* RhopH binders: RESA1, PF3D7_1201000, PF3D7_0401800, LyMP and PF3D7_1401200 (Fig. 3, 5). PF3D7_0532300 only interacted with RhopH components under weaker detergent conditions indicating this association is likely weak, transient or indirect (Fig. 3). RESA1, PF3D7_1201000, PF3D7_0401800 and LyMP all localise to the iRBC surface and have been shown previously to interact with cytoskeletal components (Fig. 5) (Foley *et al.*, 1991, Da Silva *et al.*, 1994, Silva *et al.*, 2005, Pei *et al.*, 2007, Proellocks *et al.*, 2014, Tarr *et al.*, 2014). Only RESA1 and PF3D7_1201000 showed stronger association to cytoskeletal components compared to that of the other exported proteins targeted here and therefore might be associating with RhopH components due to their localisation and not direct association (Table 1B). Cytoskeletal interaction has not been directly shown for PF3D7_1201000 but our mass spectrometry analysis shows that PF3D7_1201000 is strongly associating with spectrin, ankyrin and band 3 (Table 1B). Interestingly, PF3D7_1401200 showed the strongest association with the RhopH components, but is localised within parasite structures that partially co-localise with MCs and J-dots (Figure 1i and S2) in the iRBC and is not found at the surface like the remainder of

the five RhopH interacting proteins. Knockdown of PF3D7_1401200 resulted in a growth effect in the third cycle of GlcN treatment, where parasites displayed a delayed growth phenotype relative to 3D7 wild type parasites (Figure S7.A, B). We therefore tested sorbitol uptake after two cycles of GlcN treatment, as changes to NPP activity are observed for RhopH2 knockdown in the cycle prior to any growth effect observed (Counihan *et al.*, 2017). We observed no changes in the rate of iRBC lysis for PF3D7_1401200 compared to 3D7 control line (Figure S7.C). We were unable to study the third cycle of treatment as the parasites were younger compared to those not treated with GlcN and would therefore have less active NPPs regardless of PF3D7_1401200 association with the NPPs. Due to this, we did not further characterise the functional association of PF3D7_1401200 with RhopH components.

Mass spectrometry analysis showed that both RESA1 and PF3D7_1201000 strongly associate with MESA and PF3D7_0936800, which are known to interact with cytoskeletal components (Table 1B) (Lustigman *et al.*, 1990, Tarr *et al.*, 2014). We therefore propose that these proteins likely form a cytoskeletal (CS) complex, which serves to stabilise the RhopH complex at the iRBC cytoskeleton (Fig. 4i, 5). Interestingly PF3D7_1201000 shows a dual localisation, both at the PVM and iRBC surface, much like the RhopH components (Fig. 1i, S5C). We can therefore not exclude the possibility that PF3D7_1201000 also interacts with the RhopH complex at the PVM (Bannister *et al.*, 1986, Vincensini *et al.*, 2008, Counihan *et al.*, 2017, Ito *et al.*, 2017).

PF3D7_0532300 co-precipitated almost all of the previously identified RhopH2 binders and strongly interacted with the J-dot proteins HSP70-x, PF3D7_0801000 and HSP40s (PF3D7_0113700, PF3D7_0501100) (Table 1C and S2). PF3D7_0532300 also showed partial co-localisation with the J-dot protein PF3D7_0801000 by microscopy as well as the MC protein REX1 (Fig. 1i and S2). PF3D7_0532300 could form a transient complex with the MC resident proteins PF3D7_0301700, PF3D7_0702500 and J-dot proteins HSP70-x and

PF3D7_0801000 (Fig 4ii and 5). This complex, referred to here as the JAM complex, could serve as a trafficking hub from J-dots to MCs, as it has been previously suggested that J-dot structures serve as a bridge for exported proteins to reach the MCs (Kulzer *et al.*, 2010, Petersen *et al.*, 2016). We hypothesise that the RhopH complex could take the route from J-dots to MCs to access the iRBC surface given the interaction we observed, although formal investigation of this will be required (Sam-Yellowe *et al.*, 2001, Vincensini *et al.*, 2005, Counihan *et al.*, 2017).

In conclusion, we could not find evidence that the 13 proteins are directly involved in NPP function. We have however, successfully provided a clearer picture of the protein-protein interactions these proteins might be involved in within the iRBC (Fig. 4 and 5). As some of these proteins have not been previously tagged and studied, this also adds a new dimension to the current literature and insights into potential protein complexes and networks for future studies. This study also strengthens the link between the two trafficking structures, J-dots and MCs, and the RhopH complex suggesting it takes this route to the iRBC membrane.

Experimental procedures

Plasmid constructs

Roughly 800-1000 base pairs upstream of the stop codon of each protein was amplified from *P. falciparum* genomic DNA (gDNA) (primer sequences listed in Table S3). This recombination flank was appended with a HA-tag fused in frame with a T2A skip peptide and a neomycin resistance gene (Birnbaum *et al.*, 2017). This was followed by a *glmS* riboswitch inserted at the heterologous 3' untranslated region (UTR) of the gene (Prommana *et al.*, 2013) (Fig. S1A). Constructs used for standard recombination lacked the T2A skip peptide and neomycin resistance gene. Gene constructs were inserted into a plasmid containing human dihydrofolate reductase (hDHFR), which confers resistance to WR99210. The previously published pPTEX150-HAglmS plasmid was cut with PstI and BglII to remove the PTEX150

Accepted Article

sequence, and recombination flanks were ligated into the plasmid (de Koning-Ward *et al.*, 2009). These constructs were then transfected into 3D7 wild type parasites and placed under selection. When parasite lines were established, gDNA was extracted using DNeasy kit (Qiagen). Correct integration was confirmed by PCR, and correct size of protein by western blotting (Fig. S1B, C, D detailed methods can be found in supplementary materials).

Parasite culturing

Transgenic parasite lines were generated using standard trophozoite transfection as previously described (Fidock *et al.*, 1997). Transgenic parasites were selected for by addition of 2.5 nM WR99210, 5µg/ml blasticidin S (Sigma Aldrich), and/or 400 µg/ml G418 (geneticin, Sigma Aldrich) and maintained in culture as previously described (Trager *et al.*, 1976, Birnbaum *et al.*, 2017).

Indirect immunofluorescence assays

Infected RBCs were either dropped onto poly-L-lysine (Sigma Aldrich) coated coverslips and subsequently fixed in 4% paraformaldehyde/0.0075% glutaraldehyde for 20 min prior to quenching in 0.1M Glycine/0.1% Triton X-100, or smeared onto glass slides and fixed in ice-cold 90% acetone/10% methanol for 2 min. Cells were subsequently blocked in 3% BSA/PBS for 1 h prior to probing with primary antibodies overnight. Unbound antibodies were removed by extensive washing 0.02% TX100/PBS prior to addition of secondary antibodies (AlexaFluor) and incubated for 1 h (antibodies listed in Table S4). Washes were completed as before. Coverslips were mounted on slides with Vectorshield/DAPI. Images were obtained using Zeiss Axio Observer Z1 inverted widefield microscope or a Nikon Eclipse Ti2 microscope and processed using Fiji software. For super resolution images, a Nikon N-SIM microscope was used (extended protocol can be found in supplemented materials).

Conditional knockdown growth assays

Parasites were treated with varying concentrations of GlcN (0, 0.5, 2.5 mM) at trophozoite stage and adjusted to 1% haematocrit/0.3% parasitemia and plated in a 96-well plate in 100 μ l triplicates. Samples were taken each cycle at trophozoite stage and stored at -80°C until all samples were collected. Parasite growth was estimated by measuring lactate dehydrogenase activity as previously described (Makler *et al.*, 1993b, Persson *et al.*, 2006). Experiments were repeated on three independent occasions and completed in technical triplicates. Statistical analysis was performed on the third cycle of treatment for 2.5 mM GlcN only using an unpaired t test (with Welch correction), where growth was compared to 3D7 wild type parasites. Giemsa growth assays were prepared the same way, except smears were taken each day and stained in Giemsa stain.

Sorbitol lysis assays

Transgenic parasite lines expressing exported Nluc (Azevedo *et al.*, 2014) were sorbitol synchronised at ring stage, and the following day when the parasites were trophozoites (~32 hpi) they were treated with varying concentrations of GlcN (0, 0.5 and 2.5 mM) and plated in technical triplicates in 96-well plates at 1% haematocrit/0.5% parasitemia. In the next cycle when trophozoites (~32hpi), parasites were incubated in sorbitol lysis buffer (280 mM sorbitol, 0.1 mg/ml BSA, 20 mM Na-HEPES, pH 7.4) containing NanoGlo substrate (1:1000, Promega) and bioluminescence was monitored every 3 min by CLARIOstar BMG plate reader as described previously (Counihan *et al.*, 2017). For sorbitol lysis assays conducted after two cycles of GlcN treatment, parasites were adjusted to 1% parasitemia and 1% haematocrit on the day of the experiment. All experiments were repeated on three independent occasions and done in technical triplicates.

Reciprocal immunoprecipitation assays analysed via mass spectrometry

RBC infected with trophozoite stage parasites were either purified by passing through a magnetic column (exported proteins) or by saponin lysis (CLAG3). Pellets were lysed in 0.25% TX100 (exported proteins) or 1% Triton X-100 (CLAG3) and immunoprecipitation assays performed using commercially available anti-HA agarose beads (Sigma Aldrich). Mass spectrometry-based proteomics analysis was used to investigate protein-protein interactions for each of the immunoprecipitation assays. A detailed protocol of sample preparation and analysis can be found in the supplementary materials.

Reciprocal immunoprecipitation assays analysed via western blotting

For each tagged protein, 30 ml culture at 4% haematocrit was harvested at trophozoite stage by magnet purification. Infected RBC pellets were washed 2x in PBS containing Complete protease cocktail inhibitors (Roche) and subsequently resuspended in 1% Triton X-100/PBS lysis buffer. Cells were sonicated 2x cycles (30 s on/30 s off, Diagenode) and incubated in lysis buffer for 1 h at 4°C. Samples were centrifuged at 20 000g for 15 min at 4°C and supernatant containing solubilised proteins was incubated with anti-HA agarose beads (Sigma Aldrich) overnight at 4°C. Beads were washed 5x in lysis buffer and eluted in 1x sample buffer (6X stock: 0.3 M Tris-HCl pH 6.8, 60% glycerole, 12 mM EDTA, 12% SDS, 0.05% bromophenol blue). 100 mM DTT was added to each sample and tubes incubated at 80°C for 10 min and electrophoresed on 4-12% Bis-Tris SDS-PAGE gels (Invitrogen) in 1X MOPS buffer, prior to transferring to nitrocellulose membrane for western blotting using iBlot 1 (20V, 9 min, Invitrogen).

Acknowledgements

T.J. is a recipient of the Melbourne Research Scholarship and M.G. a recipient of a Deakin University Postgraduate Research Scholarship. T.dk-W is an NHMRC Senior Research Fellow. Special thanks to the Monash Micro Imaging facility, Micromon

Genomics Sanger Sequencing Facility, Jacobs Pharmaceuticals for WR99210, the Australian Red Cross Blood Bank for providing blood and the Bio21 Mass Spectrometry and Proteomics Facility. We thank Matthew Dixon for kindly gifting us the REX1 antibody. We thank Ben Dickerman, Smitha Sudhakar and Rasika Kumarasingha for providing technical assistance. This work was partially supported by Deakin University HAtCH funding (NC).

Conflict of interest

The authors declare no conflicts of interest.

Author contribution

T.J. carried out and designed this study, which included experimental procedure, data analysis, figures, and manuscript writing unless otherwise indicated. The 11 SLI genetic constructs were generated by P.G. and M.G. and transgenic parasite lines established by T.J. PF3D7_0501000 and PF3D7_1401200 transgenic parasite lines and PCR confirmations were done by N.C. RhopH antibodies and confirmation were generated by J.M. B.K. performed SIM microscopy and analysis. P.S. did mass spectrometry analysis using Bio21 facility for the 10 exported proteins and data was interpreted by T.J. M.G. helped with western blot immunoprecipitation assays. H.B, T.dK-W, B.C. and P.G. provided overall guidance with the study and manuscript editing.

Main figure legends

Figure 1: Localisation of the 13 exported proteins.

Localisation of the 13-tagged proteins was detected via indirect immunofluorescence assays of the trophozoite stage iRBCs, when the NPP activity is greatest. All of the HA-tagged proteins were exported into the iRBC, where i) five proteins: RESA1, 0532300, 1201000, 0401800 and LyMP showed surface localisation. Structured

Illumination Microscopy (SIM) analysis was used to obtain higher spatial resolution. PF3D7_0532300 (*) displayed either clear surface localisation, or appeared as discrete puncta at the surface and diffused throughout the iRBC cytoplasm depending on the fixation used. ii) Seven proteins showed diffuse iRBC signal resembling Maurer's clefts and showed either no, partial or complete co-localisation with the MCs marker REX1. Scale bars= 5 μm or 1 μm (SIM). Predicted domain structures of each protein are indicated to the right of their microscopy image found on PlasmoDB. 3D7 (top left) was used as negative control for HA signal (tagged protein) and EXP2 was used as PVM marker throughout. P stands for paraformaldehyde/ glutaraldehyde fixation and A for acetone/methanol fixation.

Figure 2: Conditional knockdown of the 13 proteins indicate none of the proteins are important for NPP function and only PF3D7_1401200 shows growth phenotype.

A. Western blots were performed to assess level of protein knockdown when *gImS*-tagged trophozoite stage parasites were treated with 2.5 mM glucosamine (GlcN) over one cell cycle. Densitometry was used to measure the level of protein knockdown (shown on graph), where individual blots can be found in Fig. S3A. Error bars represent SD for 2 biological replicates. **B.** Schematic of the exported Nluc reporter construct transfected into the 13 transgenic parasite lines. Nluc is N-terminally appended with the PEXEL encoding region of exported protein Hyp1 (PF3D7_0113300) and is thus exported into the iRBC. **C.** The 13 transgenic parasite lines containing exported Nluc reporter were harvested at trophozoite stage when the exported Nluc was expressed and indirect immunofluorescence assays were used to confirm that the Nluc was successfully exported into the iRBC. HA represents the target protein and Nluc represents the exported Nluc. 3D7 and RhopH2-HA*gImS* parasites containing exported Nluc were used as controls. Scale bars=5 μm . Only representative figures are shown, complete data set can be found in Fig. S3B. **D.** Trophozoite stage parasites were treated with different concentrations of GlcN. After

Accepted Article

one cycle parasites were harvested and NPP activity was assessed via sorbitol lysis assays. The percentage of sorbitol lysis measured in relative light units (RLU) released per minute of lysis is shown on the y-axis. 100% lysis was set as RLU/min in parasites not treated with GlcN. 3D7 wild type parasites (red) with an exported Nluc were used as negative control for sorbitol lysis and RhopH2-Nluc (green) are an NPP knockdown control. This data was overlaid on the RhopH2-HA binding proteins data indicated in black. None of the 13 parasite lines were found to have decreased sorbitol lysis after GlcN treatment when compared to wild type parasites. The experiment was repeated on three independent occasions, using three technical replicates and error bars represent SD. **E.** Trophozoite stage parasites were treated with different concentrations of GlcN over three consecutive parasite cycles. PF3D7_1401200 showed 50% reduction in parasite growth in the third cycle of treatment when compared to the 3D7 control. Data represent three biological replicates completed in three technical replicates. Error bars represent SD. Statistical analysis was performed using an unpaired t test (Welch's t test). The graph only shows third cycle of treatment, 2.5 mM GlcN. All cycles for individual proteins can be found in Fig. S4.

Figure 3: Reciprocal immunoprecipitations indicate five proteins out of 13 co-precipitate RhopH2.

A. Mass spectrometry analysis of the 10 proteins targeted for reciprocal immunoprecipitations revealed that only four proteins co-immunoprecipitated all RhopH components, when considering i) protein coverage (% coverage shown on the x-axis) and ii) peptide counts. Peptide numbers are shown inside coloured circles, where blue represents CLAG3 peptides, purple RhopH2 peptides and green RhopH3 peptides co-precipitated by the four proteins targeted in the assay. Thickness of the bands represents protein association, where higher peptide counts have thicker bands. RESA1 and LyMP showed the strongest association with RhopH

components whilst PF3D7_0532300 and PF3D7_1201000 showed intermediate interaction. **B.** i) Western blot analysis of reciprocal immunoprecipitations was used to confirm the mass spectrometry data, where RhopH2-HA*gImS* was used as positive control and 3D7 and PGK-HA*gImS* as negative controls. RhopH2, RESA1, PF3D7_1201000, LyMP and PF3D7_1401200 were able to co-precipitate RhopH2 in more quantity compared to control lines. * represents the target protein size. ii) GBP130 was also targeted for immunoprecipitation using IgG antibody to target native GBP130, where 3D7 incubated with beads only was used as a control. GBP130 only co-precipitated RhopH3. I; sample input, E; elution.

Figure 4: Analysis of immunoprecipitation assays reveal novel protein-protein complexes and trafficking routes within the iRBC.

i. RESA (D) and PF3D7_1201000 (E) are likely in a complex together given the similarity of their interacting partners as determined by mass spectrometry (Table 1B and S2). Both proteins interact strongly with MESA (G) and PF3D7_0936800 (F). We propose these four proteins are in a cytoskeletal (CS) complex given their interaction with cytoskeletal components and peripheral localisation within the iRBC (dotted blue circle used to highlight the complex). The degree of protein interaction is indicated by thickness of the arrows, and relevant peptide counts co-precipitated by target protein are represented at the head of the arrow (see symbols in the left panel). ii.

PF3D7_0532300 (P) and PF3D7_0301700 (Q) likely help traffic proteins within the iRBC as both proteins strongly associate with the J-dot proteins HSP70-x (N) and PF3D7_0801000 (O). These proteins also interact with the Maurer's cleft resident protein PF3D7_0702500 (R) and these five proteins could therefore form the J-dot and Maurer's cleft (JAM) complex (dotted blue circle used to highlight the complex). Proteins circled with a dotted line were not targeted for immunoprecipitation here. All peptide numbers for proteins displayed in the figure can be found in Table S2.

Figure 5: Schematic of protein networks within the iRBC

Schematic figure of protein organisation and potential protein interactions within the iRBC. **1.** From immunofluorescence assays it appears that a substantial proportion of the RhopH complex resides at the PV/PVM. This PV localisation could explain its interaction with PF3D7_0402000 (PHISTa), GBP130 and PF3D7_1201000 (PHISTb) proteins. **2.** Our data suggests that the JAM complex might help facilitate transport of proteins from J-dots to Maurer's clefts (MC). J-dot proteins strongly interacted with the RhopH components but only weak interaction was observed for MC residential proteins. It is therefore unknown as to whether the RhopH proteins are trafficked 2a) through J-dots to the MC via the JAM complex or 2b) directly from J-dots to the cytoskeleton/surface. **3.** RhopH2 and CLAG3 immunoprecipitation assays show that both components are interacting with PF3D7_1401200, a protein localised to the cytoplasm of the iRBC and could be interacting with the complex due to a trafficking role. **4.** Immunoprecipitation assays suggest that RESA1, PF3D7_1201000, MESA and PF3D7_0936800 form a cytoskeletal (CS) complex. **5.** The RhopH components could be stabilised at the iRBC membrane by the CS complex and PF3D7_0401800, however, none of the proteins appear to be individually important for the correct functioning of the NPP channels. Parasite proteins are written in black text and host cell proteins in blue text.

Table 1: Mass spectrometry analysis of reciprocal immunoprecipitation assays

A. In red are proteins targeted for reciprocal immunoprecipitation that co-precipitated RhopH component more strongly than others. **B.** Proposed cytoskeletal (CS) complex is indicated in blue. **C.** The transient J-dot and Maurer's cleft (JAM) trafficking complex is indicated in purple, with J-dot protein indicated by dark purple. 3D7-1 is control used for RhopH2 and CLAG3 assays and 3D7-2 control for exported proteins targeted. Numbers in each column represent peptides of proteins (protein names displayed vertically) co-precipitating with proteins targeted for reciprocal immunoprecipitation (protein names displayed horizontally). Extended table can be found in Table S2.

References

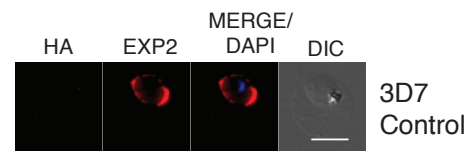
- Ahmad, M., Manzella-Lapeira, J., Saggi, G., Ito, D., Brzostowski, J.A. and Desai, S.A. (2020). Live-Cell FRET Reveals that Malaria Nutrient Channel Proteins CLAG3 and RhopH2 Remain Associated throughout Their Tortuous Trafficking. *mBio* **11**.
- Azevedo, M.F., Nie, C.Q., Elsworth, B., Charnaud, S.C., Sanders, P.R., Crabb, B.S. and Gilson, P.R. (2014). Plasmodium falciparum transfected with ultra bright NanoLuc luciferase offers high sensitivity detection for the screening of growth and cellular trafficking inhibitors. *PLoS One* **9**, e112571.
- Bannister, L.H., Mitchell, G.H., Butcher, G.A. and Dennis, E.D. (1986). Lamellar membranes associated with rhoptries in erythrocytic merozoites of Plasmodium knowlesi: a clue to the mechanism of invasion. *Parasitology* **92** (Pt 2), 291-303.
- Beck, J.R., Muralidharan, V., Oksman, A. and Goldberg, D.E. (2014). PTEX component HSP101 mediates export of diverse malaria effectors into host erythrocytes. *Nature* **511**, 592-595.
- Behl, A., Kumar, V., Bisht, A., Panda, J.J., Hora, R. and Mishra, P.C. (2019). Cholesterol bound Plasmodium falciparum co-chaperone 'PFA0660w' complexes with major virulence factor 'PfEMP1' via chaperone 'PfHsp70-x'. *Sci Rep* **9**, 2664.
- Birnbaum, J., Flemming, S., Reichard, N., Soares, A.B., Mesen-Ramirez, P., Jonscher, E., et al. (2017). A genetic system to study Plasmodium falciparum protein function. *Nat Methods* **14**, 450-456.
- Boddey, J.A. and Cowman, A.F. (2013). Plasmodium nesting: remaking the erythrocyte from the inside out. *Annu Rev Microbiol* **67**, 243-269.
- Charnaud, S.C., Dixon, M.W.A., Nie, C.Q., Chappell, L., Sanders, P.R., Nebl, T., et al. (2017). The exported chaperone Hsp70-x supports virulence functions for Plasmodium falciparum blood stage parasites. *PLoS One* **12**, e0181656.
- Cobb, D.W., Florentin, A., Fierro, M.A., Krakowiak, M., Moore, J.M. and Muralidharan, V. (2017). The Exported Chaperone PfHsp70x Is Dispensable for the Plasmodium falciparum Intraerythrocytic Life Cycle. *mSphere* **2**.
- Comeaux, C.A., Coleman, B.I., Bei, A.K., Whitehurst, N. and Duraisingh, M.T. (2011). Functional analysis of epigenetic regulation of tandem RhopH1/clag genes reveals a role in Plasmodium falciparum growth. *Mol Microbiol* **80**, 378-390.
- Cooke, B.M., Lingelbach, K., Bannister, L.H. and Tilley, L. (2004). Protein trafficking in Plasmodium falciparum-infected red blood cells. *Trends Parasitol* **20**, 581-589.
- Coppel, R.L., Lustigman, S., Murray, L. and Anders, R.F. (1988). MESA is a Plasmodium falciparum phosphoprotein associated with the erythrocyte membrane skeleton. *Mol Biochem Parasitol* **31**, 223-231.
- Counihan, N.A., Chisholm, S.A., Bullen, H.E., Srivastava, A., Sanders, P.R., Jonsdottir, T.K., et al. (2017). Plasmodium falciparum parasites deploy RhopH2 into the host erythrocyte to obtain nutrients, grow and replicate. *Elife* **6**.
- Cowman, A.F., Baldi, D.L., Healer, J., Mills, K.E., O'Donnell, R.A., Reed, M.B., et al. (2000). Functional analysis of proteins involved in Plasmodium falciparum merozoite invasion of red blood cells. *FEBS Lett* **476**, 84-88.
- Crabb, B.S., Cooke, B.M., Reeder, J.C., Waller, R.F., Caruana, S.R., Davern, K.M., et al. (1997). Targeted gene disruption shows that knobs enable malaria-infected red cells to cytoadhere under physiological shear stress. *Cell* **89**, 287-296.
- Da Silva, E., Foley, M., Dluzewski, A.R., Murray, L.J., Anders, R.F. and Tilley, L. (1994). The Plasmodium falciparum protein RESA interacts with the

- erythrocyte cytoskeleton and modifies erythrocyte thermal stability. *Mol Biochem Parasitol* **66**, 59-69.
- Davies, H.M., Thalassinou, K. and Osborne, A.R. (2016). Expansion of Lysine-rich Repeats in Plasmodium Proteins Generates Novel Localization Sequences That Target the Periphery of the Host Erythrocyte. *J Biol Chem* **291**, 26188-26207.
- Day, J., Passeecker, A., Beck, H.P. and Vakonakis, I. (2019). The Plasmodium falciparum Hsp70-x chaperone assists the heat stress response of the malaria parasite. *FASEB J* **33**, 14611-14624.
- de Koning-Ward, T.F., Dixon, M.W., Tilley, L. and Gilson, P.R. (2016). Plasmodium species: master renovators of their host cells. *Nat Rev Microbiol* **14**, 494-507.
- de Koning-Ward, T.F., Gilson, P.R., Boddey, J.A., Rug, M., Smith, B.J., Papenfuss, A.T., *et al.* (2009). A newly discovered protein export machine in malaria parasites. *Nature* **459**, 945-949.
- Dietz, O., Rusch, S., Brand, F., Mundwiler-Pachlatko, E., Gaida, A., Voss, T. and Beck, H.P. (2014). Characterization of the small exported Plasmodium falciparum membrane protein SEMP1. *PLoS One* **9**, e103272.
- Fidock, D.A. and Wellems, T.E. (1997). Transformation with human dihydrofolate reductase renders malaria parasites insensitive to WR99210 but does not affect the intrinsic activity of proguanil. *Proc Natl Acad Sci U S A* **94**, 10931-10936.
- Foley, M., Tilley, L., Sawyer, W.H. and Anders, R.F. (1991). The ring-infected erythrocyte surface antigen of Plasmodium falciparum associates with spectrin in the erythrocyte membrane. *Mol Biochem Parasitol* **46**, 137-147.
- Gilson, P.R., Chisholm, S.A., Crabb, B.S. and de Koning-Ward, T.F. (2017). Host cell remodelling in malaria parasites: a new pool of potential drug targets. *Int J Parasitol* **47**, 119-127.
- Ginsburg, H., Kutner, S., Krugliak, M. and Cabantchik, Z.I. (1985). Characterization of permeation pathways appearing in the host membrane of Plasmodium falciparum infected red blood cells. *Mol Biochem Parasitol* **14**, 313-322.
- Heiber, A., Kruse, F., Pick, C., Gruring, C., Flemming, S., Oberli, A., *et al.* (2013). Identification of new PNEPs indicates a substantial non-PEXEL exportome and underpins common features in Plasmodium falciparum protein export. *PLoS Pathog* **9**, e1003546.
- Hernand, P., Ciceron, L., Pionneau, C., Vaquero, C., Combadiere, C. and Deterre, P. (2016). Plasmodium falciparum proteins involved in cytoadherence of infected erythrocytes to chemokine CX3CL1. *Sci Rep* **6**, 33786.
- Ito, D., Schureck, M.A. and Desai, S.A. (2017). An essential dual-function complex mediates erythrocyte invasion and channel-mediated nutrient uptake in malaria parasites. *Elife* **6**.
- Kaneko, O., Tsuboi, T., Ling, I.T., Howell, S., Shirano, M., Tachibana, M., *et al.* (2001). The high molecular mass rhoptry protein, RhopH1, is encoded by members of the clag multigene family in Plasmodium falciparum and Plasmodium yoelii. *Mol Biochem Parasitol* **118**, 223-231.
- Kaneko, O., Yim Lim, B.Y., Iriko, H., Ling, I.T., Otsuki, H., Grainger, M., *et al.* (2005). Apical expression of three RhopH1/Clag proteins as components of the Plasmodium falciparum RhopH complex. *Mol Biochem Parasitol* **143**, 20-28.
- Kilili, G.K., Shakya, B., Dolan, P.T., Wang, L., Husby, M.L., Stahelin, R.V., *et al.* (2019). The Plasmodium falciparum MESA erythrocyte cytoskeleton-binding (MEC) motif binds to erythrocyte ankyrin. *Mol Biochem Parasitol* **231**, 111189.
- Kirk, K. and Horner, H.A. (1995). Novel anion dependence of induced cation transport in malaria-infected erythrocytes. *J Biol Chem* **270**, 24270-24275.
- Kirk, K., Horner, H.A., Elford, B.C., Ellory, J.C. and Newbold, C.I. (1994). Transport of diverse substrates into malaria-infected erythrocytes via a pathway

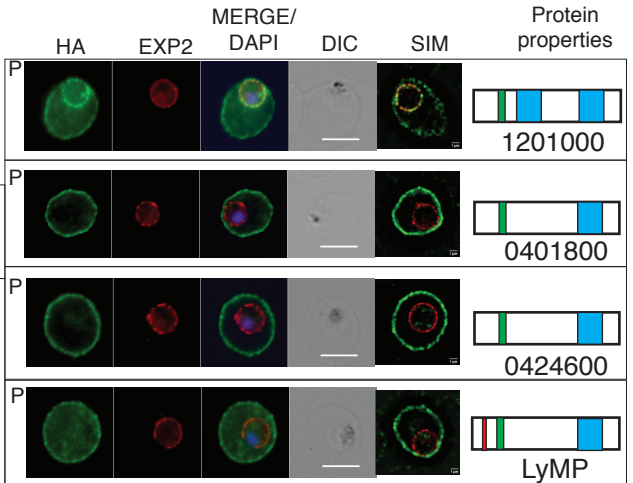
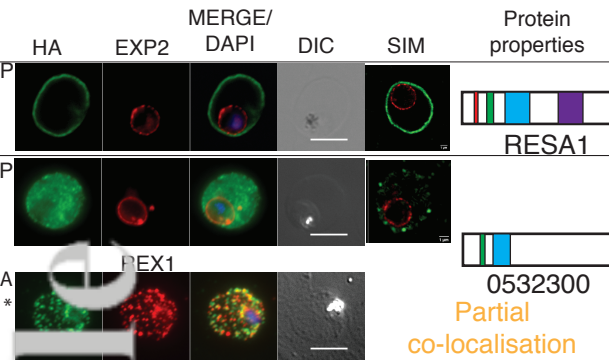
- showing functional characteristics of a chloride channel. *J Biol Chem* **269**, 3339-3347.
- Kulzer, S., Charnaud, S., Dagan, T., Riedel, J., Mandal, P., Pesce, E.R., *et al.* (2012). Plasmodium falciparum-encoded exported hsp70/hsp40 chaperone/co-chaperone complexes within the host erythrocyte. *Cell Microbiol* **14**, 1784-1795.
- Kulzer, S., Rug, M., Brinkmann, K., Cannon, P., Cowman, A., Lingelbach, K., *et al.* (2010). Parasite-encoded Hsp40 proteins define novel mobile structures in the cytosol of the P. falciparum-infected erythrocyte. *Cell Microbiol* **12**, 1398-1420.
- Lanzer, M., Wickert, H., Krohne, G., Vincensini, L. and Braun Breton, C. (2006). Maurer's clefts: a novel multi-functional organelle in the cytoplasm of Plasmodium falciparum-infected erythrocytes. *Int J Parasitol* **36**, 23-36.
- Lew, V.L., Tiffert, T. and Ginsburg, H. (2003). Excess hemoglobin digestion and the osmotic stability of Plasmodium falciparum-infected red blood cells. *Blood* **101**, 4189-4194.
- Lustigman, S., Anders, R.F., Brown, G.V. and Coppel, R.L. (1990). The mature-parasite-infected erythrocyte surface antigen (MESA) of Plasmodium falciparum associates with the erythrocyte membrane skeletal protein, band 4.1. *Mol Biochem Parasitol* **38**, 261-270.
- Magowan, C., Coppel, R.L., Lau, A.O., Moronne, M.M., Tchernia, G. and Mohandas, N. (1995). Role of the Plasmodium falciparum mature-parasite-infected erythrocyte surface antigen (MESA/PfEMP-2) in malarial infection of erythrocytes. *Blood* **86**, 3196-3204.
- Maier, A.G., Rug, M., O'Neill, M.T., Brown, M., Chakravorty, S., Szeszak, T., *et al.* (2008). Exported proteins required for virulence and rigidity of Plasmodium falciparum-infected human erythrocytes. *Cell* **134**, 48-61.
- Makler, M.T. and Hinrichs, D.J. (1993a). Measurement of the lactate dehydrogenase activity of Plasmodium falciparum as an assessment of parasitemia. *Am J Trop Med Hyg* **48**, 205-210.
- Makler, M.T., Ries, J.M., Williams, J.A., Bancroft, J.E., Piper, R.C., Gibbins, B.L. and Hinrichs, D.J. (1993b). Parasite lactate dehydrogenase as an assay for Plasmodium falciparum drug sensitivity. *Am J Trop Med Hyg* **48**, 739-741.
- McHugh, E., Carmo, O.M.S., Blanch, A., Looker, O., Liu, B., Tiash, S., *et al.* (2020). Role of Plasmodium falciparum Protein GEXP07 in Maurer's Cleft Morphology, Knob Architecture, and P. falciparum EMP1 Trafficking. *mBio* **11**.
- Moreira, C.K., Naissant, B., Coppi, A., Bennett, B.L., Aime, E., Franke-Fayard, B., *et al.* (2016). The Plasmodium PHIST and RESA-Like Protein Families of Human and Rodent Malaria Parasites. *PLoS One* **11**, e0152510.
- Nguiragool, W., Bokhari, A.A., Pillai, A.D., Rayavara, K., Sharma, P., Turpin, B., *et al.* (2011). Malaria parasite clag3 genes determine channel-mediated nutrient uptake by infected red blood cells. *Cell* **145**, 665-677.
- Oberli, A., Slater, L.M., Cutts, E., Brand, F., Mundwiler-Pachlatko, E., Rusch, S., *et al.* (2014). A Plasmodium falciparum PHIST protein binds the virulence factor PfEMP1 and comigrates to knobs on the host cell surface. *FASEB J* **28**, 4420-4433.
- Parish, L.A., Mai, D.W., Jones, M.L., Kitson, E.L. and Rayner, J.C. (2013). A member of the Plasmodium falciparum PHIST family binds to the erythrocyte cytoskeleton component band 4.1. *Malar J* **12**, 160.
- Pei, X., Guo, X., Coppel, R., Bhattacharjee, S., Haldar, K., Gratzer, W., *et al.* (2007). The ring-infected erythrocyte surface antigen (RESA) of Plasmodium falciparum stabilizes spectrin tetramers and suppresses further invasion. *Blood* **110**, 1036-1042.
- Perkins, M. (1988). Stage-dependent processing and localization of a Plasmodium falciparum protein of 130,000 molecular weight. *Exp Parasitol* **65**, 61-68.

- Persson, K.E., Lee, C.T., Marsh, K. and Beeson, J.G. (2006). Development and optimization of high-throughput methods to measure *Plasmodium falciparum*-specific growth inhibitory antibodies. *J Clin Microbiol* **44**, 1665-1673.
- Petersen, W., Kulzer, S., Engels, S., Zhang, Q., Ingmundson, A., Rug, M., *et al.* (2016). J-dot targeting of an exported HSP40 in *Plasmodium falciparum*-infected erythrocytes. *Int J Parasitol* **46**, 519-525.
- Proellocks, N.I., Herrmann, S., Buckingham, D.W., Hanssen, E., Hodges, E.K., Elsworth, B., *et al.* (2014). A lysine-rich membrane-associated PHISTb protein involved in alteration of the cytoadhesive properties of *Plasmodium falciparum*-infected red blood cells. *FASEB J* **28**, 3103-3113.
- Prommana, P., Uthaipibull, C., Wongsombat, C., Kamchonwongpaisan, S., Yuthavong, Y., Knuepfer, E., *et al.* (2013). Inducible knockdown of *Plasmodium* gene expression using the glmS ribozyme. *PLoS One* **8**, e73783.
- Saliba, K.J. and Kirk, K. (2001). Nutrient acquisition by intracellular apicomplexan parasites: staying in for dinner. *Int J Parasitol* **31**, 1321-1330.
- Sam-Yellowe, T.Y., Fujioka, H., Aikawa, M., Hall, T. and Drazba, J.A. (2001). A *Plasmodium falciparum* protein located in Maurer's clefts underneath knobs and protein localization in association with Rhop-3 and SERA in the intracellular network of infected erythrocytes. *Parasitol Res* **87**, 173-185.
- Sargeant, T.J., Marti, M., Caler, E., Carlton, J.M., Simpson, K., Speed, T.P. and Cowman, A.F. (2006). Lineage-specific expansion of proteins exported to erythrocytes in malaria parasites. *Genome Biol* **7**, R12.
- Schulze, J., Kwiatkowski, M., Borner, J., Schluter, H., Bruchhaus, I., Burmester, T., *et al.* (2015). The *Plasmodium falciparum* exportome contains non-canonical PEXEL/HT proteins. *Mol Microbiol* **97**, 301-314.
- Sherling, E.S., Knuepfer, E., Brzostowski, J.A., Miller, L.H., Blackman, M.J. and van Ooij, C. (2017). The *Plasmodium falciparum* rhopty protein RhopH3 plays essential roles in host cell invasion and nutrient uptake. *Elife* **6**.
- Siddiqui, G., Proellocks, N.I. and Cooke, B.M. (2020). Identification of essential exported *Plasmodium falciparum* protein kinases in malaria-infected red blood cells. *Br J Haematol* **188**, 774-783.
- Silva, M.D., Cooke, B.M., Guillotte, M., Buckingham, D.W., Sauzet, J.P., Le Scanf, C., *et al.* (2005). A role for the *Plasmodium falciparum* RESA protein in resistance against heat shock demonstrated using gene disruption. *Mol Microbiol* **56**, 990-1003.
- Sleeb, B.E., Lopaticki, S., Marapana, D.S., O'Neill, M.T., Rajasekaran, P., Gazdik, M., *et al.* (2014). Inhibition of Plasmeprin V activity demonstrates its essential role in protein export, PfEMP1 display, and survival of malaria parasites. *PLoS Biol* **12**, e1001897.
- Staines, H.M., Rae, C. and Kirk, K. (2000). Increased permeability of the malaria-infected erythrocyte to organic cations. *Biochim Biophys Acta* **1463**, 88-98.
- Tarr, S.J., Moon, R.W., Hardege, I. and Osborne, A.R. (2014). A conserved domain targets exported PHISTb family proteins to the periphery of *Plasmodium* infected erythrocytes. *Mol Biochem Parasitol* **196**, 29-40.
- Tiburcio, M., Dixon, M.W., Looker, O., Younis, S.Y., Tilley, L. and Alano, P. (2015). Specific expression and export of the *Plasmodium falciparum* Gametocyte EXported Protein-5 marks the gametocyte ring stage. *Malar J* **14**, 334.
- Tilley, L., Dixon, M.W. and Kirk, K. (2011). The *Plasmodium falciparum*-infected red blood cell. *Int J Biochem Cell Biol* **43**, 839-842.
- Trager, W. and Jensen, J.B. (1976). Human malaria parasites in continuous culture. *Science* **193**, 673-675.
- Upston, J.M. and Gero, A.M. (1995). Parasite-induced permeation of nucleosides in *Plasmodium falciparum* malaria. *Biochim Biophys Acta* **1236**, 249-258.

- Vincensini, L., Fall, G., Berry, L., Blisnick, T. and Braun Breton, C. (2008). The RhopH complex is transferred to the host cell cytoplasm following red blood cell invasion by *Plasmodium falciparum*. *Mol Biochem Parasitol* **160**, 81-89.
- Vincensini, L., Richert, S., Blisnick, T., Van Dorsselaer, A., Leize-Wagner, E., Rabilloud, T. and Braun Breton, C. (2005). Proteomic analysis identifies novel proteins of the Maurer's clefts, a secretory compartment delivering *Plasmodium falciparum* proteins to the surface of its host cell. *Mol Cell Proteomics* **4**, 582-593.
- W.H.O (2020) World Malaria Report 2020. Geneva: World Health Organisation.
- Wagner, M.A., Andemariam, B. and Desai, S.A. (2003). A two-compartment model of osmotic lysis in *Plasmodium falciparum*-infected erythrocytes. *Biophys J* **84**, 116-123.
- Waller, K.L., Nunomura, W., An, X., Cooke, B.M., Mohandas, N. and Coppel, R.L. (2003). Mature parasite-infected erythrocyte surface antigen (MESA) of *Plasmodium falciparum* binds to the 30-kDa domain of protein 4.1 in malaria-infected red blood cells. *Blood* **102**, 1911-1914.
- Zhang, M., Wang, C., Otto, T.D., Oberstaller, J., Liao, X., Adapa, S.R., *et al.* (2018). Uncovering the essential genes of the human malaria parasite *Plasmodium falciparum* by saturation mutagenesis. *Science* **360**.
- Zhang, Q., Ma, C., Oberli, A., Zinz, A., Engels, S. and Przyborski, J.M. (2017). Proteomic analysis of exported chaperone/co-chaperone complexes of *P. falciparum* reveals an array of complex protein-protein interactions. *Sci Rep* **7**, 42188.



i. Localised to iRBC surface



ii. Diffuse/punctate localisation within iRBC

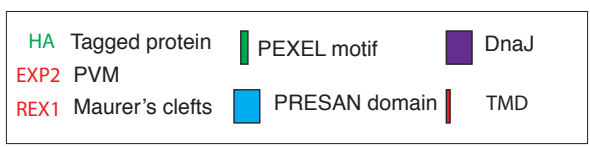
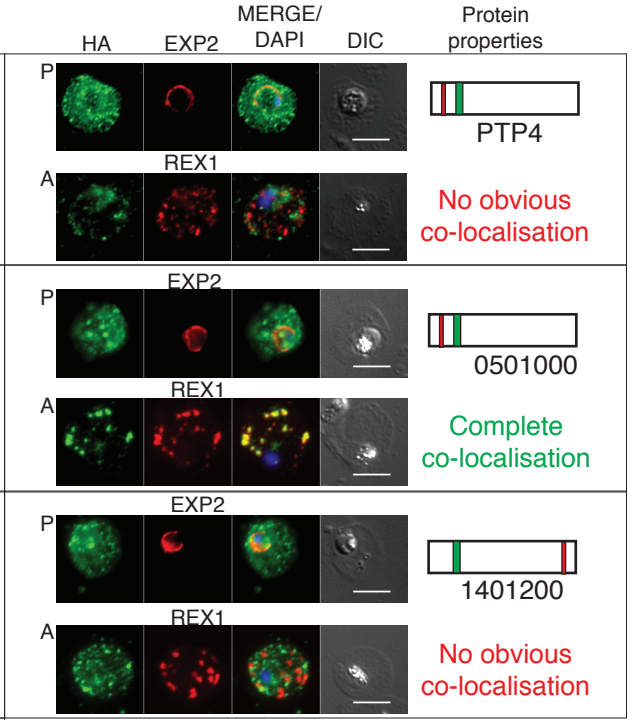
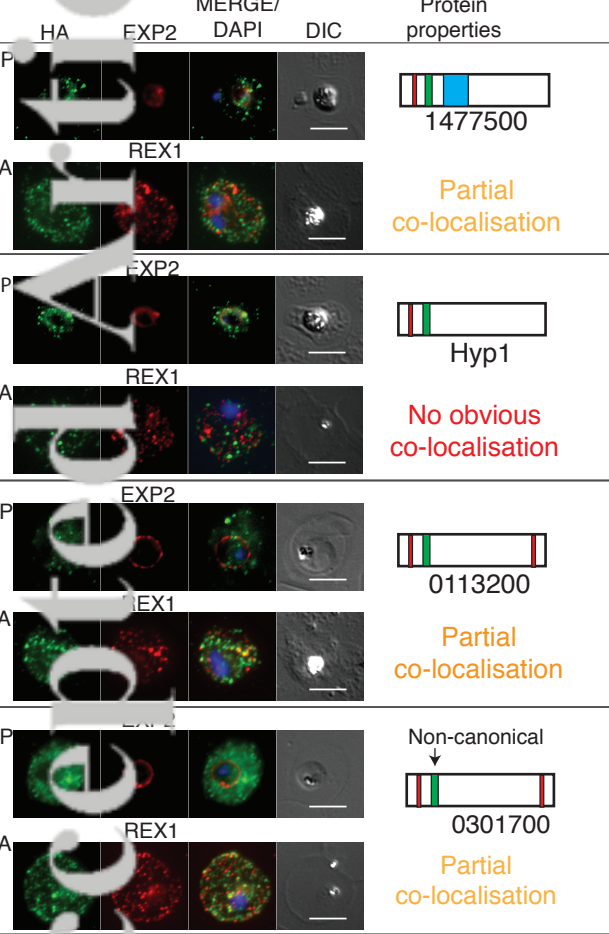


Figure 1

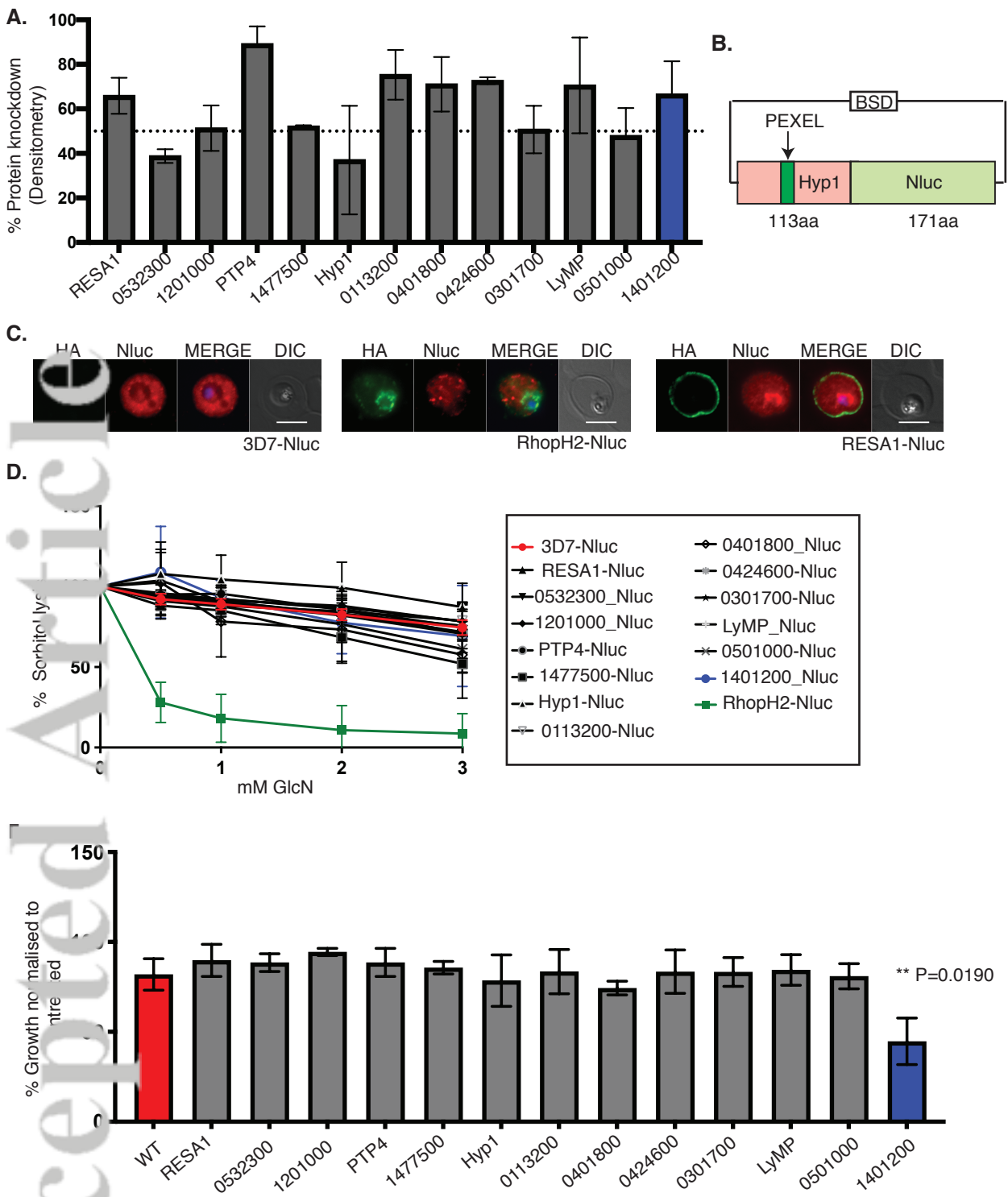
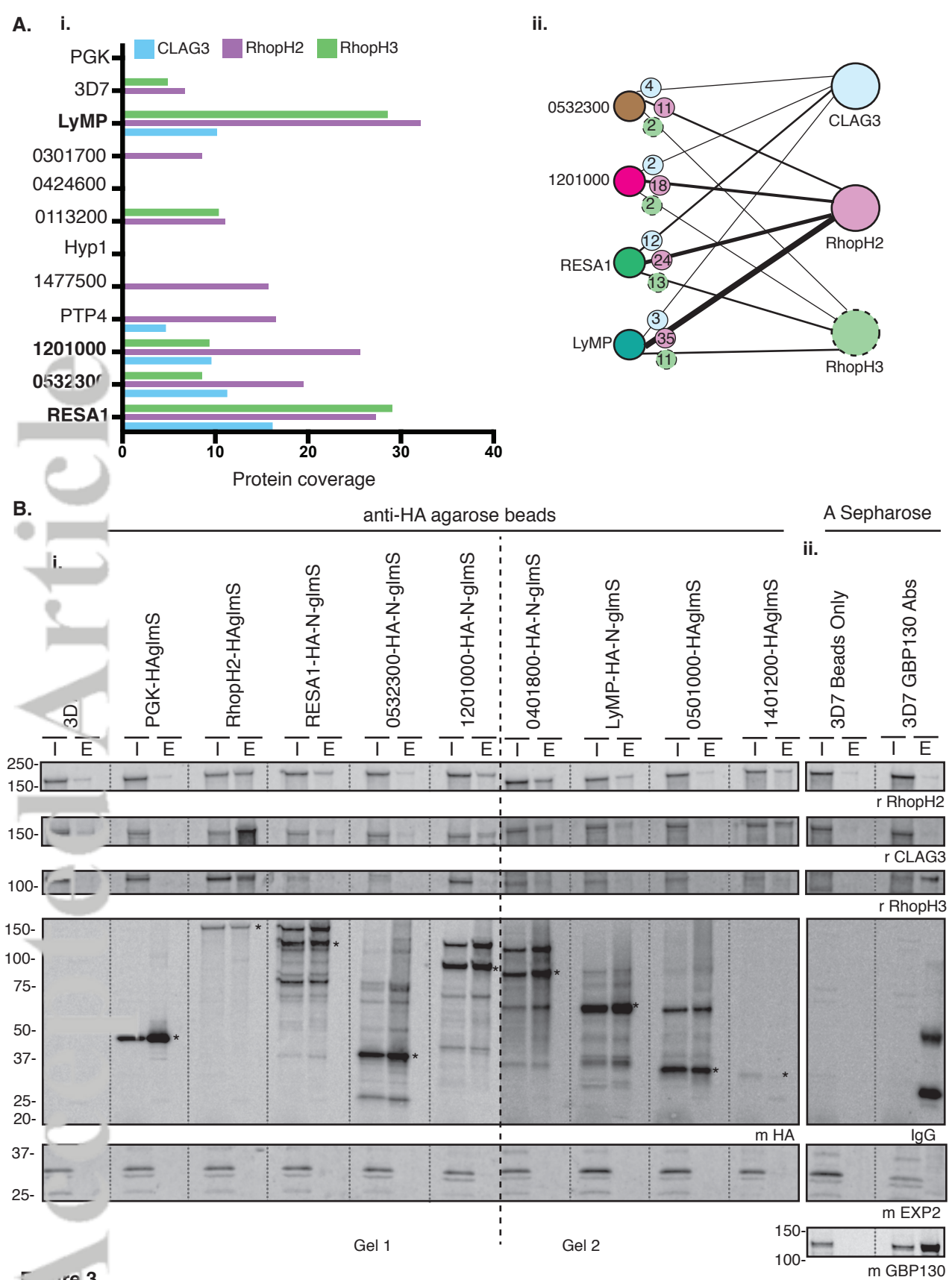
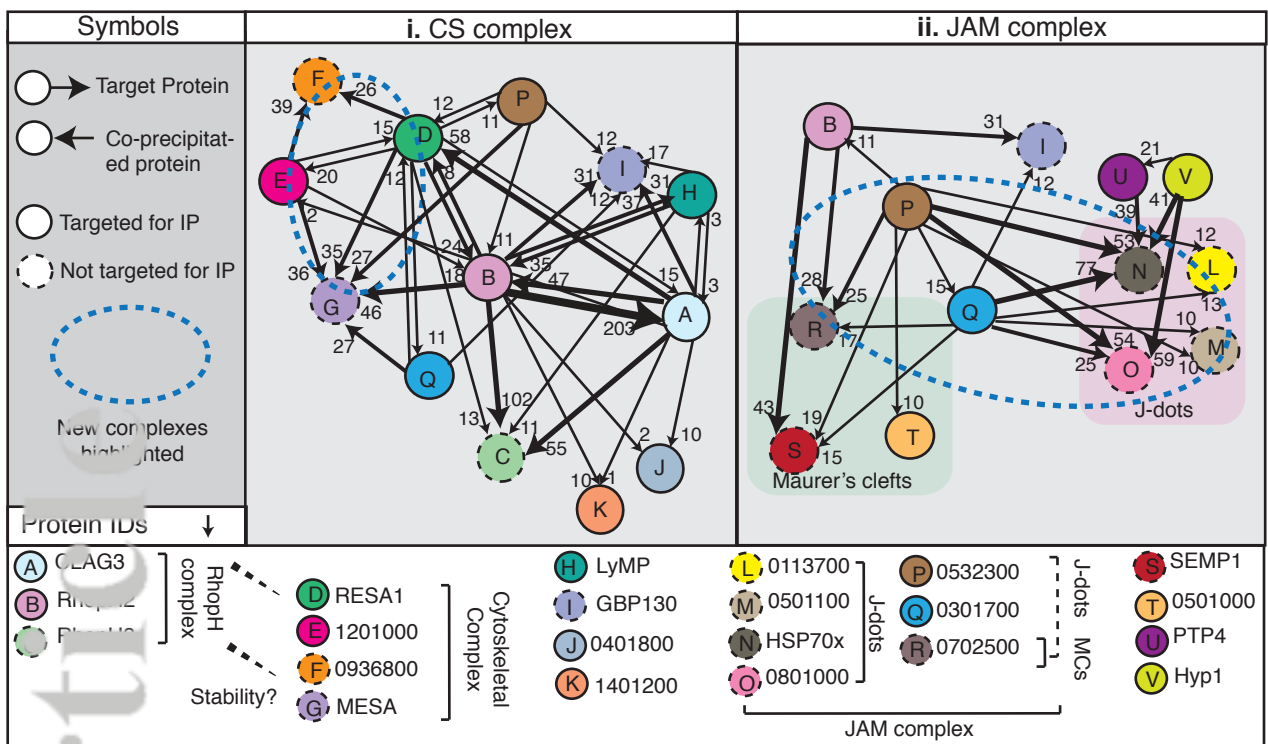


Figure 2





Fig

Accepted Article

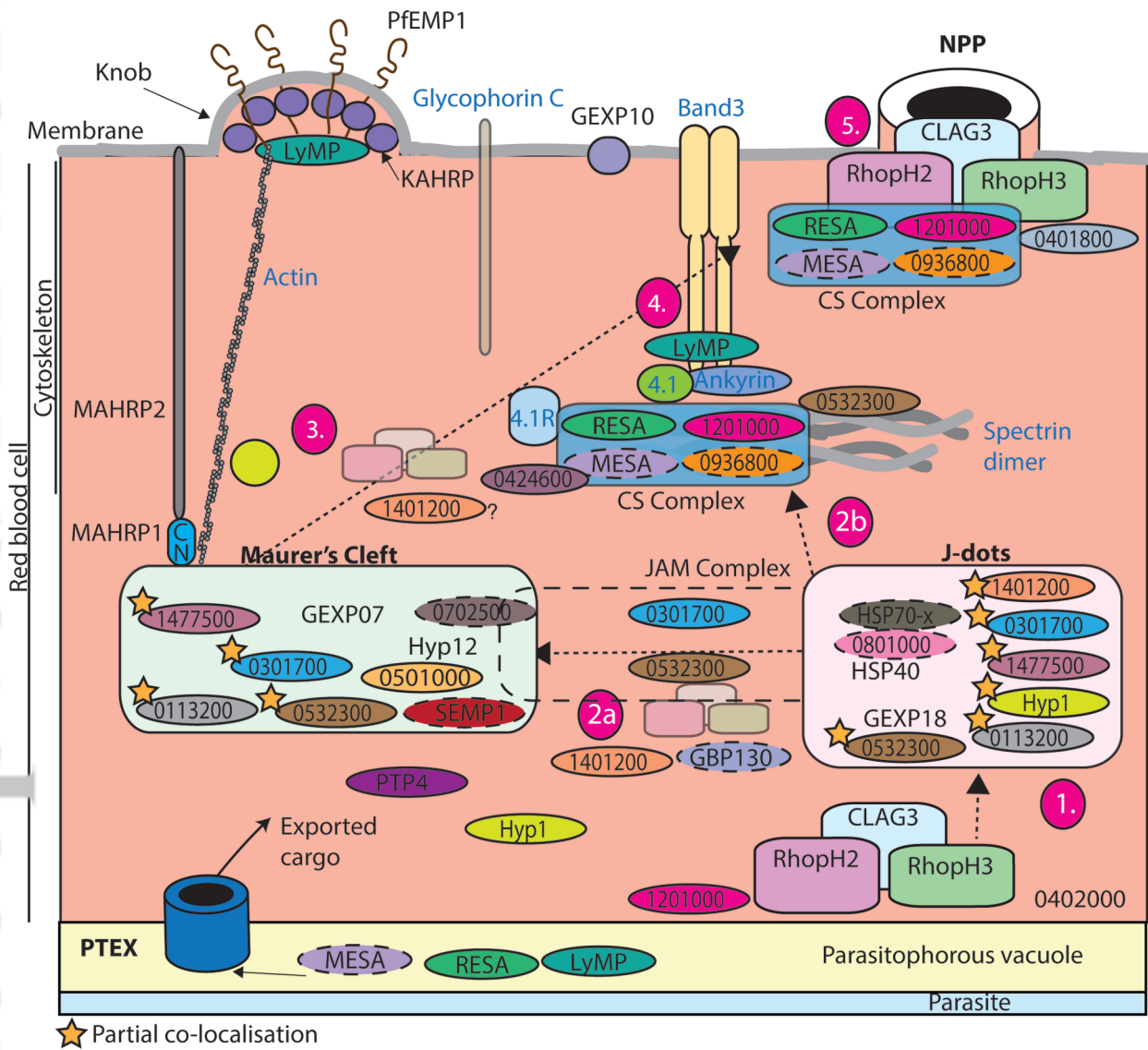


Figure 5

CMI_13332_Fig 5.tif

Table 1: Mass spectrometry analysis of reciprocal immunoprecipitation assays

A.

Interacting proteins ↓	Proteins targeted for immunoprecipitation								
	RhopH2	CLAG3	3D7-1	RESA1	0532300	1201000	LyMP	3D7-2	PGK
CLAG3	203	319	12	15	4	2	3	1	0
RhopH2	48	47	9	24	11	18	35	1	0
RhopH3	102	55	12	13	2	2	11	1	0
RESA1	8	58	7	92	12	13	0	0	0
0532300	3	0	0	11	26	6	0	2	1
1201000	3	2	0	20	5	44	0	0	1
LyMP	31	3	2	12	12	10	58	5	1
0401800	2	11	4	10	8	5	2	1	0
1401200	10	1	0	1	6	1	0	0	0

B.

Interacting proteins ↓	Proteins targeted for immunoprecipitation						
	RhopH2	CLAG3	3D7-1	RESA1	1201000	3D7-2	PGK
RESA1	8	58	7	92	13	0	0
1201000	3	2	0	20	44	0	1
MESA	46	9	3	35	36	8	1
0936800	6	0	0	26	39	0	0
Ankyrin	173	220	78	163	134	7	0
Spectrin	116	512	100	377	600	11	10
Band 3	49	90	15	50	33	2	0

C.

Interacting proteins ↓	Proteins targeted for immunoprecipitation					
	RhopH2	CLAG3	3D7-1	0532300	0301700	3D7-2
0113700	0	0	0	12	13	0
0501100	0	0	0	10	10	0
HSP70x	23	37	21	53	77	13
0801000	22	1	0	54	24	5
0532300	3	0	0	26	2	2
0301700	2	0	0	15	22	4
0702500	28	0	0	25	17	1